Article

Expansion by Contraction: Diversifying the Photochemical Reactivity Scope of Diazo-oxochlorins toward Development of *in Situ* Alkylating Agents

Tillmann Ko#pke, Maren Pink, and Jeffrey M. Zaleski

J. Am. Chem. Soc., **2008**, 130 (47), 15864-15871 • DOI: 10.1021/ja800094e • Publication Date (Web): 31 October 2008

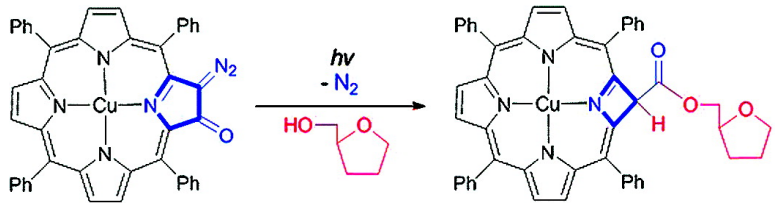

More About This Article

Additional resources and features associated with this article are available within the HTML version:

- Supporting Information
- Access to high resolution figures
- Links to articles and content related to this article
- Copyright permission to reproduce figures and/or text from this article

View the Full Text HTML

J|A|C|S
ARTICLES

Published on Web 10/31/2008

Expansion by Contraction: Diversifying the Photochemical Reactivity Scope of Diazo-oxochlorins toward Development of *in Situ* Alkylating Agents

Tillmann Köpke, Maren Pink, and Jeffrey M. Zaleski*

Department of Chemistry, Indiana University, Bloomington, Indiana 47405

Received January 5, 2008; E-mail: zaleski@indiana.edu

Abstract: Irradiation of 2-diazo-3-oxochlorins (200 W, $\lambda \geq 345$ nm, 10 °C) in the presence of nucleophilic and biomimetic substrates 1-butanol, tosylhydrazine, or tetrahydrofurfuryl alcohol generates Wolff-rearranged, pyrrole ring-contracted azeteoporphyrinoids in 11−34% yield, with the corresponding hydroxyporphyrins in up to 55% yield. For metalated diazo-oxochlorins, these products compete with intramolecular exocyclic ring formation by *meso*-phenyl ring addition, which occurs in up to 76% yield in the absence of substrate. The dependence of product distribution on substrate is established by photolysis in neat dichlorometane. Under these conditions, formation of the Wolff-rearranged product is inhibited and the phenyl addition product dominates (76%) due to the absence of a good nucleophile. A conceptually analogous dependence is also observed for the free-base derivative, with the exocyclic ring-containing dimerization product isolated in 42% yield. The third reaction pathway, formation of the hydroxyporphyrin, is enhanced by the presence of non-nucleophilic, oxidizable substrates such as 1,4-cyclohexadiene (M = Cu; 55%); however, in the presence of the bulky and oxidatively more stable *tert*-butyl alcohol, intramolecular exocyclic ring-quenching is observed in 51% yield with no detection of the hydroxyporphyrin. X-ray structure characterization of the azeteoporphyrinoids reveals a planar macrocycle, illustrating the strong influence of periphery contraction. Specifically, the copper-containing azeteoporphyrinoids show remarkably short Cu−N_{azete} distances of 1.88−1.90 Å. All porphyrinoid photoproducts possess intense absorption bands throughout the visible spectral region, indicating that ring-contracted substrate adducts, as well as phenyl ring addition products, maintain porphyrinoid aromaticity. Overall, the ability of these chromophores to photochemically react under substrate control may make unimolecular porphyrinoid photoreagents such as these useful for applications in photobiology or O_2-independent photodynamic therapy.

Introduction

DNA alkylation is one of the prominent modes of action of potent natural products (e.g., mitomycins,[1−6] duocarmycins,[7,8] acylfulvenes[9−11]) involved in drug development. Although structurally distinct, the kinamycin family[12,13] of the diazobenzo[*b*]fluorene antibiotics are functionally related due to their ability to alkylate biological substrates. The kinamycins and glycosylated, dimeric lomaiviticin A and B constructs (Figure 1) are proposed to function by loss of N_2 from a terminal diazo unit. They are effective against Gram-positive bacteria, and kinamycins A and C have been shown to inhibit growth of both

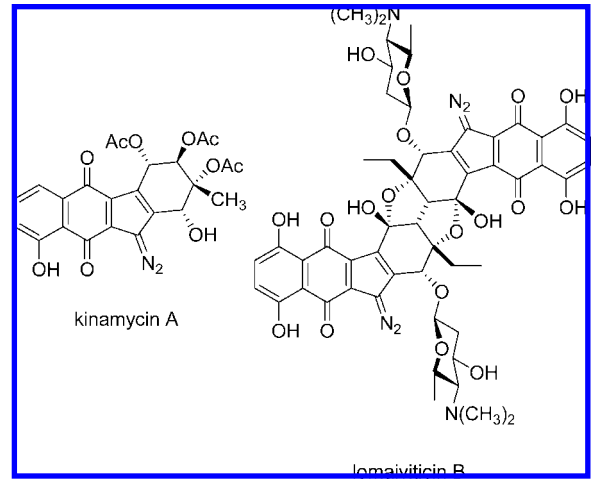

Figure 1. Diazobenzo[*b*]fluorene natural products kinamycin A and dimeric lomaiviticin B.

(1) Galm, U.; Hager, M. H.; Van Lanen, S. G.; Ju, J.; Thorson, J. S.; Shen, B. *Chem. Rev.* **2005**, *105*, 739.
(2) Kohn, H.; Hong, Y. P. *J. Am. Chem. Soc.* **1990**, *112*, 4596.
(3) Kumar, G. S.; Musser, S. M.; Cummings, J.; Tomasz, M. *J. Am. Chem. Soc.* **1996**, *118*, 9209.
(4) Li, V. S.; Kohn, H. *J. Am. Chem. Soc.* **1991**, *113*, 275.
(5) Peterson, D. M.; Fisher, J. *Biochemistry* **1986**, *25*, 4077.
(6) Tomasz, M.; Lipman, R.; Verdine, G. L.; Nakanishi, K. *Biochemistry* **1986**, *25*, 4337.
(7) Boger, D. L.; Boyce, C. W.; Garbaccio, R. M.; Goldberg, J. A. *Chem. Rev.* **1997**, *97*, 787.
(8) Tichenor, M. S.; Trzupek, J. D.; Kastrinsky, D. B.; Shiga, F.; Hwang, I.; Boger, D. L. *J. Am. Chem. Soc.* **2006**, *128*, 15683.
(9) Blunt, J. W.; Copp, B. R.; Munro, M. H. G.; Northcote, P. T.; Prinsep, M. R. *Nat. Prod. Rep.* **2003**, *20*, 1.
(10) Gong, J.; Vaidyanathan, V. G.; Yu, X.; Kensler, T. W.; Peterson, L. A.; Sturla, S. J. *J. Am. Chem. Soc.* **2007**, *129*, 2101.
(11) McMorris, T. C. *Bioorg. Med. Chem.* **1999**, *7*, 881.
(12) Gould, S. J. *Chem. Rev.* **1997**, *97*, 2499.
(13) Hasinoff, B. B.; Wu, X.; Yalowich, J. C.; Goodfellow, V.; Laufer, R. S.; Adedayo, O.; Dmitrienko, G. I. *Anti-Cancer Drugs* **2006**, *17*, 825.

10.1021/ja800094e CCC: $40.75

Chinese hamster ovary and K562 cells,[13] while in the broader NCI 60-cell screen, kinamycin C reveals high nanomolar IC_{50} values similar to the potent antitumor agent mitomycin C. The homodimer lomaiviticin A also exhibits activity against Gram-positive bacteria and a variety of tumor cell lines, with IC_{50} values ranging from 0.7 to 6.0 nM.[14] Despite these studies, and the luxury of synthetic access to the kinamycin natural products,[15] the precise mechanism of biological activity is still not fully understood. However, it is generally accepted that the reaction pathway responsible for cell growth inhibition involves formation of a primary radical species via N_2 loss.[13,14] Along with the enediyne natural products,[16] the diazoparaquinone antibiotics are a rare example of intramolecular diradical generation via mild activation.

The uniqueness of N_2 release as an entropically driven trigger for reactivity leads to several potential biological applications for diazo analogues that include nuclease activity,[17−23] photoaffinity labeling,[24−38] and photodynamic therapy (PDT).[39,40] The formation of toxic radicals without the need for O_2[41] suggests that such compounds could be an alternative to traditional, $^1O_2$-mediated PDT for hypoxic environments. Carbenes formed by N_2 loss can undergo alkylation reactions via the singlet intermediates, or H-atom abstraction from external substrates usually via the triplet state.[42−44] Additionally, if the loss of dinitrogen occurs from a α-diazo ketone framework, the electron-deficient carbene can facilitate intramolecular Wolff rearrangement,[45,46] which results in a transient ketene that adds nucleophiles.[47,48] In this sense, biology provides a variety of potential nucleophiles such as the sugar backbone of DNA and other basic substrates.

With these motivations, we are pursuing the development and diradical reactivity of diazo-oxochlorin chromophores.[49−53] Due to their intense absorption bands throughout the visible spectral region,[54,55] porphyrins and chlorins are routinely employed as effective photosensitizers for $^1O_2$ formation in PDT. Consequently, improved synthetic strategies have led to the development of porphyrinoids with modulated optical[56−59] and electronic properties.[53,60−62] By combining the electronic features of such chromophores with the alklyation, H-atom abstraction, or Wolff reactivity of the diazo-moiety, novel porphyrin photoreagents may be accessible.

Herein we describe the photoreactivity of diazo-oxochlorins in the presence of nucleophilic substrates. Broadband photolysis generates an initial carbene intermediate that differentiates reactivity on the basis of the availability of nucleophile. In the presence of substrates, the unique, ring-contracted azeteoporphyrin−substrate adducts are obtained, while in their absence, exocyclic ring formation and H-atom abstraction dominate the product distribution. Photochemically initiated and controlled addition chemistry of this type may ultimately find utility in photobiological labeling and alkylation applications.

Results

Syntheses. The diazo-oxochlorins were prepared via published methodology.[51] Briefly, reaction of the corresponding metalated dioxochlorin precursors and tosylhydrazine in the presence of $Zn(OAc)_2$ (1 equiv) in dichloromethane results in their generation in good yields (**Ni1**, 64%; **Cu1**, 73%). Demetalation with

(14) Feldman, K. S.; Eastman, K. J. *J. Am. Chem. Soc.* **2005**, *127*, 15344.
(15) Lei, X.; Porco, J. A., Jr. *J. Am. Chem. Soc.* **2006**, *128*, 14790.
(16) Rawat, D. S.; Zaleski, J. M. *Synlett* **2004**, 393.
(17) Behr, J. P. *J. Chem. Soc., Chem. Commun.* **1989**, 101.
(18) Daidone, G.; Maggio, B.; Plescia, S.; Raffa, D.; Musiu, C.; Milia, C.; Perra, G.; Marongiu, M. E. *Eur. J. Med. Chem.* **1998**, *35*, 375.
(19) Hiramoto, K.; Kaku, M.; Sueyoshi, A.; Fujise, M.; Kikugawa, K. *Chem. Res. Toxicol.* **1995**, *8*, 356.
(20) Nakatani, K.; Maekawa, S.; Tanabe, K.; Saito, I. *J. Am. Chem. Soc.* **1995**, *117*, 10635.
(21) Nakatani, K.; Shirai, J.; Sando, S.; Saito, I. *Tetrahedron Lett.* **1997**, *38*, 6047.
(22) Nielsen, P. E.; Jeppesen, C.; Egholm, M.; Buchardt, O. *Nucleic Acids Res.* **1988**, *16*, 3877.
(23) Wu, F.; Bergstrom, M.; Stridsberg, M.; Orlefors, H.; Eriksson, B.; Oberg, K.; Watanabe, Y.; Langstrom, B. *Anticancer Res.* **1997**, *17*, 2363.
(24) Blanton, M. P.; Dangott, L. J.; Raja, S. K.; Lala, A. K.; Cohen, J. B. *J. Biol. Chem.* **1998**, *273*, 8659.
(25) DeGraw, A. J.; Zhao, Z.; Strickland, C. L.; Taban, A. H.; Hsieh, J.; Jefferies, M.; Xie, W.; Shintani, D. K.; McMahan, C. M.; Cornish, K.; Distefano, M. D. *J. Org. Chem.* **2007**, *72*, 4587–4595.
(26) Fagart, J.; Sobrio, F.; Marquet, A. *J. Labelled Compds. Radiopharm.* **1997**, *39*, 791.
(27) Fisher, A.; Mann, A.; Verma, V.; Thomas, N.; Mishra, R. K.; Johnson, R. L. *J. Med. Chem.* **2006**, *49*, 307.
(28) Fisher, A. L. Photoaffinity labeling and macrocyclic spiro bicyclic analogs of the dopamine receptor modulator L-prolyl-L-leucyl-glycinamide. Ph.D. Thesis, University of Minnesota, 2005.
(29) Gartner, C. A. *Curr. Med. Chem.* **2003**, *10*, 671.
(30) Hosoya, T.; Hiramatsu, T.; Ikemoto, T.; Aoyama, H.; Ohmae, T.; Endo, M.; Suzuki, M. *Bioorg. Med. Chem. Lett.* **2005**, *15*, 1289.
(31) Hosoya, T.; Hiramatsu, T.; Ikemoto, T.; Nakanishi, M.; Aoyama, H.; Hosoya, A.; Iwata, T.; Maruyama, K.; Endo, M.; Suzuki, M. *Org. Biomol. Chem.* **2004**, *2*, 637.
(32) Kan, T.; Kita, Y.; Morohashi, Y.; Tominari, Y.; Hosoda, S.; Tomita, T.; Natsugari, H.; Iwatsubo, T.; Fukuyama, T. *Org. Lett.* **2007**, *9*, 2055.
(33) Kim, E. Y. L.; Gronewold, C.; Chatterjee, A.; Von der Lieth, C.-W.; Kliem, C.; Schmauser, B.; Wiessler, M.; Frei, E. *ChemBioChem* **2005**, *6*, 422.
(34) Knorre, D. G.; Godovikova, T. S. *FEBS Lett.* **1998**, *433*, 9.
(35) Lebedeva, N. A.; Rechkunova, N. I.; Khodyreva, S. N.; Favre, A.; Lavrik, O. I. *Biochem. Biophys. Res. Commun.* **2002**, *297*, 714.
(36) Nagase, T.; Shinkai, S.; Hamachi, I. *Chem. Commun.* **2001**, 229.
(37) Palmer, B. D.; Henare, K.; Woon, S.-T.; Sutherland, R.; Reddy, C.; Wang, L.-C. S.; Kieda, C.; Ching, L.-M. *J. Med. Chem.* **2007**, *50*, 3757.
(38) Pandurangi, R. S.; Lusiak, P.; Kuntz, R. R.; Volkert, W. A.; Rogowski, J.; Platz, M. S. *J. Org. Chem.* **1998**, *63*, 9019.
(39) Detty, M. R.; Gibson, S. L.; Wagner, S. J. *J. Med. Chem.* **2004**, *47*, 3897–3915.
(40) Jasat, A.; Dolphin, D. *Chem. Rev.* **1997**, *97*, 2267.
(41) Szacilowski, K.; Macyk, W.; Drzewiecka-Matuszek, A.; Brindell, M.; Stochel, G. *Chem. Rev.* **2005**, *105*, 2647.
(42) Wentrup, C. *Reactive Molecules*; John Wiley and Sons: New York, 1984333.
(43) Bourissou, D.; Guerret, O.; Gabbaie, F. P.; Bertrand, G. *Chem. Rev.* **2000**, *100*, 39.
(44) Tomioka, H. *Acc. Chem. Res.* **1997**, *30*, 315.
(45) Bogdanova, A.; Popik, V. V. *J. Am. Chem. Soc.* **2004**, *126*, 11293.
(46) Urdabayev, N. K.; Popik, V. V. *J. Am. Chem. Soc.* **2004**, *126*, 4058.
(47) Ye, T.; McKervey, M. A. *Chem. Rev.* **1994**, *94*, 1091.
(48) Kirmse, W. *Eur. J. Org. Chem.* **2002**, 2193.
(49) Cavaleiro, J. A. S.; Gerdan, V. M.; Hombrecher, H. K.; Neves, M. G. P. M. S.; Silva, A. M. S. *Heterocycl. Commun.* **1997**, *3*, 253.
(50) Hombrecher, H. K.; Gerdan, V. M.; Cavaleiro, J. A. S.; Neves, M. G. P. M. S. *Heterocycl. Commun.* **1997**, *3*, 453.
(51) Köpke, T.; Pink, M.; Zaleski, J. M. *Synlett* **2006**, 2183.
(52) Köpke, T.; Pink, M.; Zaleski, J. M. *Org. Biomol. Chem.* **2006**, *4*, 4059.
(53) Köpke, T.; Pink, M.; Zaleski, J. M. *Chem. Commun.* **2006**, 4940.
(54) Holten, D.; Bocian, D. F.; Lindsey, J. S. *Acc. Chem. Res.* **2002**, *35*, 57.
(55) Sessler, J. L.; Seidel, D. *Angew. Chem., Int. Ed.* **2003**, *42*, 5134.
(56) Nath, M.; Huffman, J. C.; Zaleski, J. M. *J. Am. Chem. Soc.* **2003**, *125*, 11484.
(57) Nath, M.; Pink, M.; Zaleski, J. M. *J. Am. Chem. Soc.* **2005**, *127*, 478.
(58) Aihara, H.; Jaquinod, L.; Nurco, D. J.; Smith, K. M. *Angew. Chem., Int. Ed.* **2001**, *40*, 3439.
(59) Shen, D.-M.; Liu, C.; Chen, Q.-Y. *Chem. Commun.* **2005**, 4982.
(60) Crossley, M. J.; King, L. G. *J. Chem. Soc., Chem. Commun.* **1984**, 920.
(61) Lara, K. K.; Rinaldo, C. R.; Brückner, C. *Tetrahedron* **2005**, *61*, 2529.
(62) Chandra, T.; Kraft, B. J.; Huffman, J. C.; Zaleski, J. M. *Inorg. Chem.* **2003**, *42*, 5158.

Scheme 1. Summary of Reaction Products Generated by Broadband Photolysis of 2-Diazo-3-oxo-5,10,15,20-tetraphenylchlorins

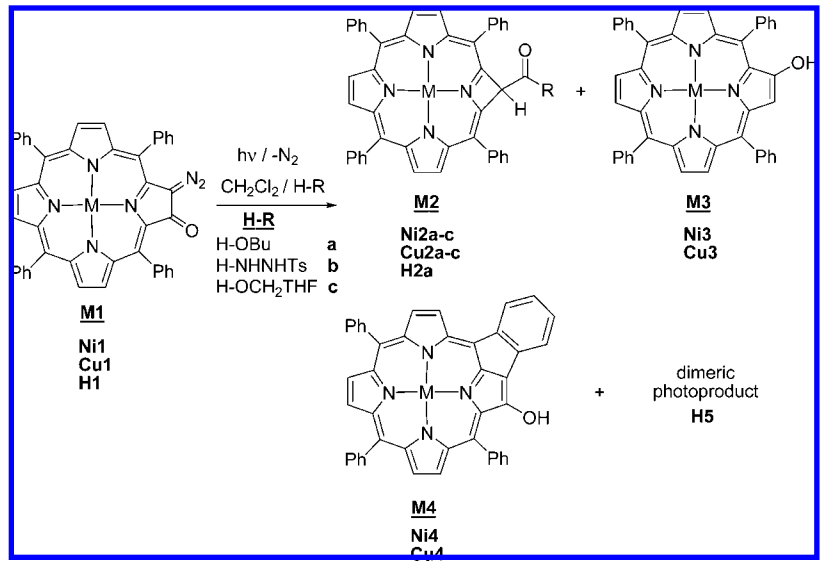

Table 1. Experimental Conditions and Isolated Yields for Broadband Photolysis of Diazo-oxochlorins

			photolysis product yield (%)					
expt[a]	M1	substrate	M2a	M2b	M2c	M3	M4	H5
1	**Ni1**	BuOH (**a**)	16			29	12	
2		Ts-NH-NH_2 (**b**)		11		6	76	
3		FurfurylOH (**c**)			28	35	12	
4		−				trace	76	
5	**Cu1**	BuOH (**a**)	14			43	6	
6		Ts-NH-NH_2 (**b**)		13		18	60	
7		FurfurylOH (**c**)			16	55	6	
8						6	66	
9	**H1**	BuOH (**a**)	34					10
10								42

[a] Photolysis experiments: expt 1, 15 mg/20 mL, CH_2Cl_2:**a** 1:4 (v/v), 9 h; expt 2, 15 mg/20 mL, CH_2Cl_2:**b** (10 equiv), 9 h; expt 3, 15 mg/20 mL, CH_2Cl_2:**c** 1:4 (v/v), 9 h; expt 4, 15 mg/20 mL, CH_2Cl_2, 9 h; expt 5, 20 mg/20 mL, CH_2Cl_2:**a** 1:4 (v/v), 6 h; expt 6, 20 mg/20 mL, CH_2Cl_2:**b** (10 equiv), 6 h; expt 7, 20 mg/20 mL, CH_2Cl_2:**c** 1:4 (v/v), 6 h; expt 8, 20 mg/20 mL, CH_2Cl_2, 6 h; expt 9, 20 mg/20 mL, CH_2Cl_2:**a** 1:4 (v/v), 9 h; expt 10, 10 mg/10 mL, CH_2Cl_2, 9 h.

concentrated H_2SO_4 produces the free-base analogue (**H1**) straightforwardly in 90%.

Photochemistry. In the presence of nucleophiles (1-butanol, tosylhydrazine, tetrahydrofurfuryl alcohol), photolysis of diazo-oxochlorins (**M1**) in dichloromethane solution yields four molecular products upon nitrogen extrusion (Scheme 1). These have been isolated and characterized as the remarkable Wolff-rearranged azeteoporphyrin (**M2a**−**c**, 16−28%), the bimolecularly derived 2-hydroxyporphyrin (**M3**, 29−55%), and the intramolecular exocyclic ring-containing hydroxyporphyrinoid (**M4**, 6−76%), as well as a dimerization product (**H5**, 10%) in the case of the free-base derivative only. The observed product ratios are strongly influenced by the concentration of nucleophile in the reaction (Table 1). For photolysis of **Ni1** and **Cu1** undertaken in the dichloromethane solution in the presence of nucleophillic substrates (experiments 1−3, 5−7, and 9, Table 1), the unprecedented nucleophile adduct is isolated as a key product, along with the 2-hydroxyporphyrin (**M3**) or the intramolecular ring-addition product (**M4**). Depending upon reaction conditions, one of these latter two species is the primary photochemical product isolated. Interestingly, in the absence of nucleophile (experiments 4 and 8, Table 1), only the unimolecular quenching product **M4** is obtained in high yield (66−76%). In contrast, photolysis of **H1** in the presence of 1-butanol as a nucleophilic substrate generates adduct **H2a** in 34% yield, along with 10% of a new species, the dimeric radical−radical coupling product of two exocyclic ring-containing monomers (**H5**). For photoreactions devoid of nucleophile, this dimeric species dominates and is obtained in as high as 42% yield. Isolation of the metalated hydroxyporphyrinoids **M3** and **M4**, as well as free-base dimer **H5**, mandates that the Wolff rearrangement competes with several intra- and intermolecular photochemical reaction pathways.

Since one of the proposed mechanisms for reaction of the diazobenzo[*b*]fluorene natural products with DNA involves alkylation of the nucleic acid substrate,[14] diazo-oxochlorins **Ni1** and **Cu1** were photolyzed in the presence of tetrahydrofurfuryl alcohol. The five-membered cyclic alcohol resembles the backbone of biological substrates based on a carbohydrate scaffold (e.g., DNA, RNA), as well as the aminoglycoside antibiotics (e.g., neomycin B) which are widely used for the treatment of a variety of infections, including tuberculosis and pneumonia.[63] In this latter case, a successful adduct may have potential as an optical probe for mechanistic drug/cell interactions.

When **Ni1** and **Cu1** are photolyzed in the presence of tetrahydrofurfuryl alcohol, substrate adducts **Ni2c** (28%) and **Cu2c** (16%) are isolated as polar porphyrinoids, along with the expected **Ni3** (35%) and **Cu3** (55%) products from a possible H-atom abstraction pathway (experiments 3 and 7, Table 1). The presence of **Ni3** and **Cu3** in pronounced yields indicates that carbene quenching by purported H-atom abstraction (*vide infra*) is strongly competitive with substrate−adduct formation.

X-ray Characterization of Photoproducts. Addition of nucleophilic substrate clearly mitigates the observed product distribution. Molecular structures of pyrrole ring-contracted porphyrinoids that contain butoxy and tosyl ester functionality on the porphyrinoid ring periphery are illustrated in Figure 2. The three molecular structures each exhibit strict planarity of

(63) Quader, S.; Boyd, S. E.; Jenkins, I. D.; Houston, T. A. *J. Org. Chem.* **2007**, *72*, 1962.

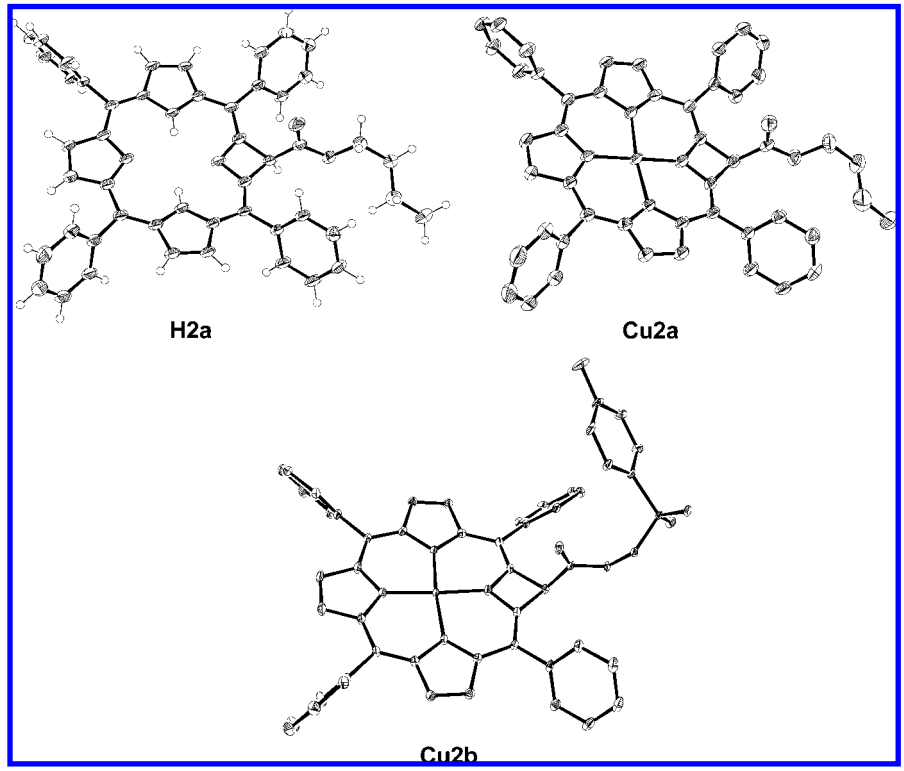

Figure 2. X-ray crystal structures of photoproducts **H2a**, **Cu2a**, and **Cu2b**. For **Cu2a** and **Cu2b**, H-atoms are omitted for clarity.

the π-conjugated macrocycle. The observation is notable since Cu-containing porphyrinoids are often weakly distorted from planarity.[64] These findings are in agreement with our communication[52] in which the planar methanol adduct was reported to be generated under similar conditions, further supporting the proposal that the four-membered azete ring dictates the conformation of the porphyrinoid product. For **Cu2a**, the Cu−N_{azete} distance is 1.887(3) Å, shorter than the remaining Cu−N bonds in the center of the macrocycle (1.93−2.00 Å) but very similar to the Cu−N_{azete} distance of 1.889(3) Å of the methoxy ester analogue.[52] The X-ray structure of **H2a** reveals similar structural parameters and the additional insight that the butyl group is disordered over two sites (ratio 88:12). The structures in Figure 2 illustrate that, for **Cu2a** and **H2a**, 1-butanol attacks the ketene intermediate via the O−H bond, while for **Cu2b**, tosylhydrazine adds through the nitrogen lone pair, indicating the tolerance of the ketene reaction to different electronic nucleophiles. Under comparable photolysis conditions, tetrahydrofurfuryl alcohol adds to the chlorin periphery in a manner similar to that observed with 1-butanol, resulting in an X-ray structure analogous to those of the ester adducts (Figure 3). The molecular structure of **Cu2c** also exhibits a short Cu−N_{azete} distance of 1.900(4) Å characteristic of the unusual azeteoporphyrin, while the remaining Cu−N bonds range between 1.93 and 2.00 Å and are more typical of porphyrinoid structures.[64,65]

In addition to the remarkable scaffolds of the substrate adducts, the molecular structures of monomeric (**Cu4**) and dimeric (**H5**) intramolecular ring-addition products are shown in Figure 4. The connectivities of the individual porphyrinoid

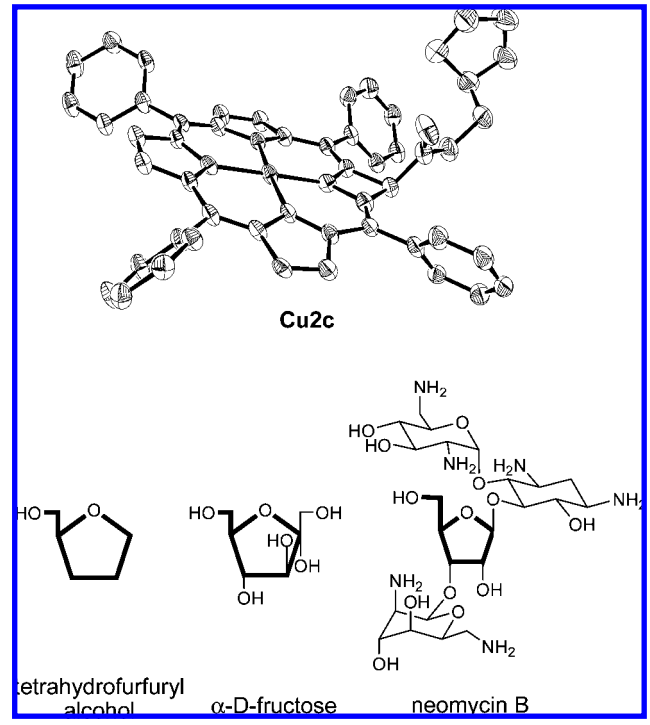

Figure 3. Top: X-ray crystal structure of **Cu2c** (H-atoms are omitted for clarity). Bottom: Tetrafurfuryl alcohol substrate **c** and analogues.

units are identical and vary only in the hybridization of the perimeter functionality (OH vs C═O). Photoinduced radical addition across the *meso*-phenyl ring produces the intramolecularly quenched monomer, which can further react by either H-atom abstraction or bimolecular radical−radical coupling to generate **Cu4** or **H5**, respectively. Crystallographically, porphyrin **Cu4** is disordered over two positions with about 0.86

(64) Henling, L. M.; Schaefer, W. P.; Hodge, J. A.; Hughes, M. E.; Gray, H. B. *Acta Crystallogr., Sect. C: Cryst. Struct. Commun.* **1993**, *C49*, 1743.
(65) Kaufmann, T.; Shamsai, B.; Lu, R. S.; Bau, R.; Miskelly, G. M. *Inorg. Chem.* **1995**, *34*, 5073.

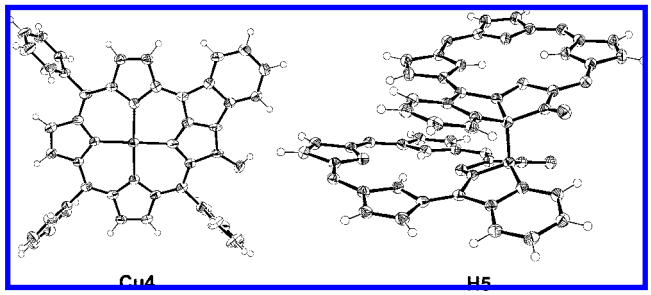

Figure 4. X-ray structure of photoproduct **Cu4**, exibiting exocyclic ring formation (left), and dimeric free-base photoproduct **H5**, which derives from intramolecular quenching and subsequent radical−radical coupling reaction (right). The phenyl rings in **H5** have been omitted for clarity.

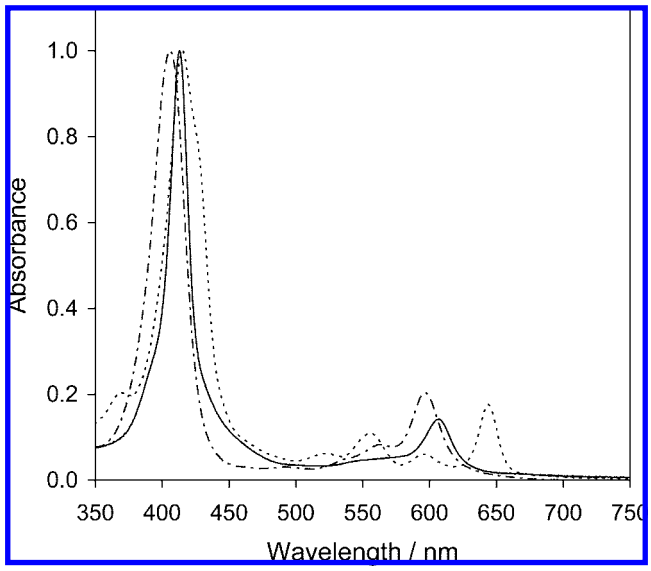

Figure 5. Normalized electronic spectra of Wolff-rearranged photoproducts **Ni2a** (− • −), **Cu2a** (—), and **H2a** (- - -) in CH_2Cl_2.

ether solvent molecule per formula unit. The X-ray structure of the free-base dimer **H5** reveals that the carbons connecting the two macrocycles possess sp^3 hybridization and are the central atoms of a distorted tetrahedron, with this 1.63 Å bond considerably elongated relative to the remaining three C−C distances (1.50−1.54 Å). The structure also includes the solvents ether and dichloromethane in the formula unit. Two ether molecules are disordered over a special position, one of which is additionally disordered with dichloromethane.

Electronic Spectra. The normalized electronic spectra of **Ni2a**, **Cu2a**, and **H2a** are shown in Figure 5. These unusual azeteoporphyrin products exhibit electronic spectra in CH_2Cl_2 that qualitatively resemble those of the corresponding 2-diazo-3-oxochlorin precursors in energy and intensity, with strong Soret absorption between $\lambda = 400$ and 415 nm and a prominent Q_x band at long wavelength ($\lambda = 580-640$ nm). The metalated forms also show a weaker vibronic overtone to higher energy of Q_x, while **H2a** exhibits the customary Q_y band at $\lambda = 555$ nm and associated overtone at $\lambda = 525$ nm. These observed spectral differences for **Ni2a**, **Cu2a**, and **H2a** are in agreement with the classical electronic structure description (i.e., symmetry, orbital degeneracy) of the conjugated 20-electron π-system of the macrocycle.[66] For substrate adducts **Ni2a**−**c** and **Cu2a**−**c**, the electronic spectra within the respective series are almost

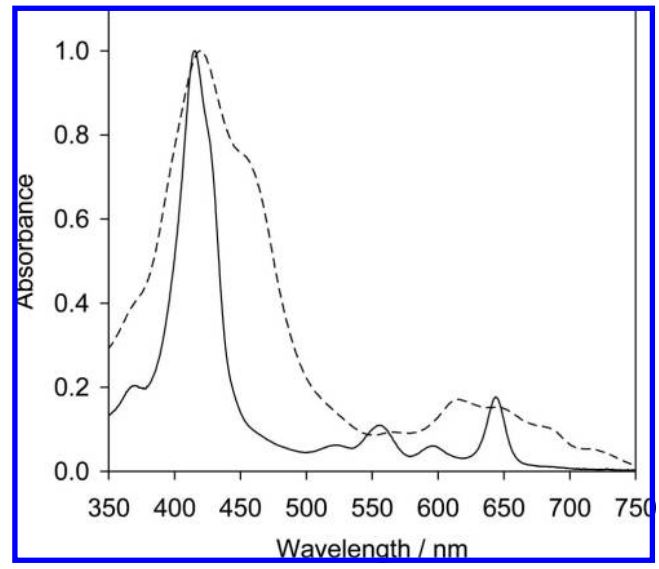

Figure 6. Comparison of normalized electronic spectra of photoproducts **H2a** (—) and **H5** (- - -) in CH_2Cl_2.

identical. The λ_{max} (Soret) ranges between 404 and 407 nm and λ_{max} (Q_x) between 594 and 598 nm for **Ni2a**−**c**, while for **Cu2a**−**c**, λ_{max} (Soret) = 412 nm and λ_{max} (Q_x) is centered at 603−605 nm. In light of the variability in substrate, the insensitivity of the electronic properties to substrate addition indicates that the 20-electron π-system is uncoupled from the C_β position of the azete ring, as predicted for chlorins by the Gouterman model.[67]

Comparison of the electronic spectra of **H2a** and the dimeric structure **H5** (Figure 6) reveals a pronounced broadening of both the Soret and Q-band features and a marked red-shift of the lowest energy components of the electronic spectral envelope. The Soret band maximum is nearly degenerate with the **H2a** monomer; however, a second feature of comparable intensity is now predominant at $\lambda = 457$ nm. Accompanying these transitions are at least five clearly defined absorption maxima at $\lambda = 565$, 612, 642, 679, and 715 nm, spanning a Q-region of $\sim$5000 cm^{-1}. These electronic properties are a direct consequence of the new exocyclic rings in each monomer formed by electrophilic aromatic substitution of the carbene intermediate with the adjacent *meso*-phenyl group, as well as the short intermacrocyle distance (3.03−4.11 Å) caused by the direct $C_\beta-C_\beta$ bond (1.63 Å) between the monomers (i.e., exciton coupling).

Aqueous Micelle-Encapsulated Photochemistry. The desire to impart control over the photoreactivity of the diazo-oxochlorins, coupled with an interest in moving toward aqueous solution photochemistry, led to encapsulation of **Cu1** into micelles of 16:0 PEG3 PE. Photolysis ($\lambda \geq 345$ nm) of an aqueous solution of 0.013×10^{-6} M micelle-encapsulated **Cu1** results in isosbestic conversion to a new species with $\lambda_{max} =$ 414 and 537 nm within 10 min, which was subsequently identified and characterized as the hydroxyporphyrin derivative **Cu3** (Figure 7a). In contrast, photolysis of a dichloromethane solution of 0.016×10^{-6} M **Cu1** results in multiple and consecutive photochemical decay pathways, as evidenced by the rapid disappearance of the starting material with $\lambda_{max} = 435$ and 620 nm and growth of new features at $\lambda_{max} = 416$, 465,

(66) Eisner, U.; Linstead, R. P. *J. Chem. Soc.* **1955**, 3749.

(67) Gouterman, M. In *The Porphyrins*; Dolphin, D., Ed.; Academic Press, Inc: New York, 1978; Vol. III, p 1.

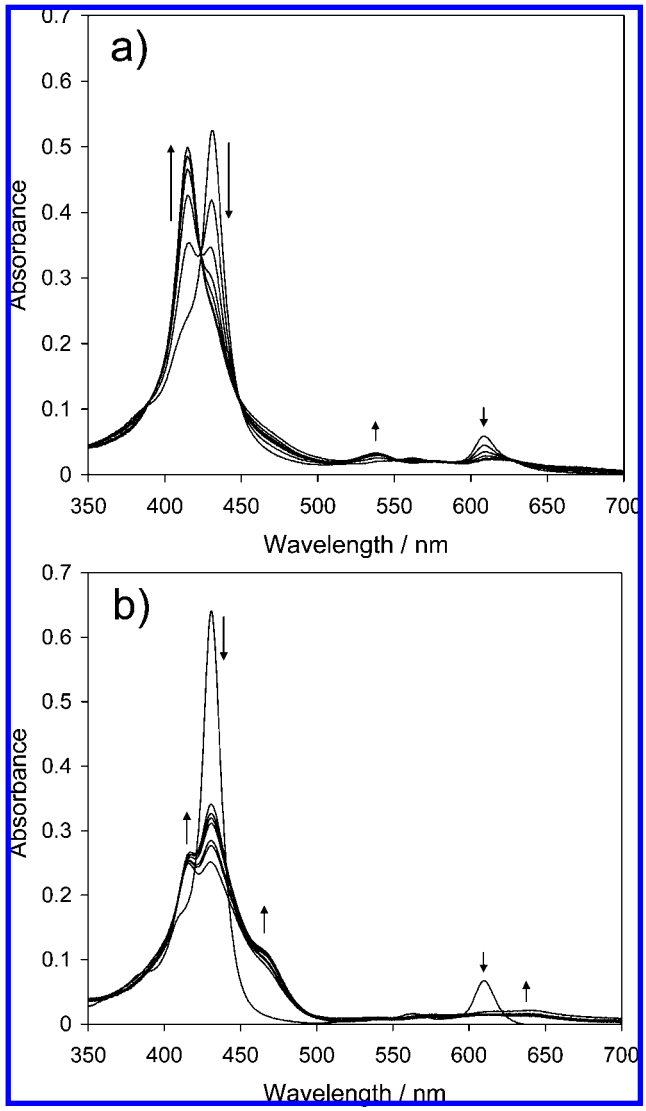

Figure 7. Photolysis of **Cu1** at $\lambda \geq 345$ nm in (a) an aqueous micelle-encapsulated environment and (b) CH_2Cl_2. Spectra were monitored in (a) after 30 s, 60 s, 90 s, 2 min, 4 min, and 10 min of photolysis; spectra were obtained in (b) at 3, 5, 15, 30, 50, 70, and 120 min photolysis times.

and 638 nm (Figure 7b). The multicomponent reaction and product distribution mirrors the photochemical solution experiments that lead to a suite of isolated products in Scheme 1, thereby verifying the presence of primary bimolecular photochemical reaction pathways in free solution.

Discussion

The diverse photochemical product distribution is clearly symptomatic of competing carbene reaction mechanisms that depend intimately upon the presence of substrate. Photolysis of **M1** leads to immediate loss of N_2 and formation of a carbene diradical, as illustrated in Scheme 2 for **Cu1**. Based on the absence of a detectable $S = 1$ EPR signal at low temperatures,[52] as well as carbene-derived olefin photoproducts from triplet−triplet coupling,[43,44,68,69] this initial species (ignoring the spin on the central copper) is tentatively assigned as a singlet spin system (**Cu1S**). Within this spin manifold, there exist three possible

Scheme 2. Proposed Mechanism for Photoproduct Formation upon Irradiation of **Cu1**

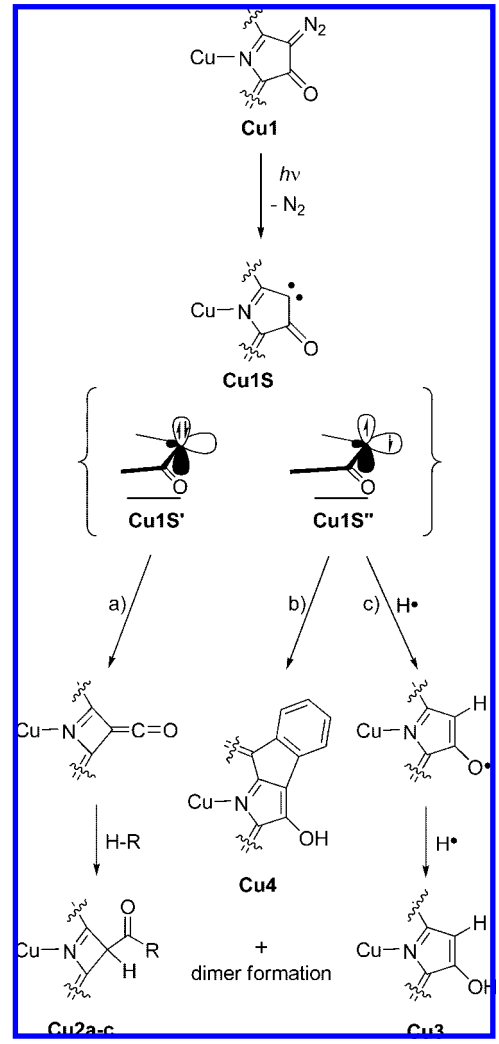

orbital states where the spin-paired electrons can reside: (1) both electrons occupy the p_z atomic orbital on the carbon atom with an empty in-plane sp^2 hybrid orbital (**Cu1S′**); (2) one electron each in the p_z and the orthogonal sp^2 hybrid orbitals, resulting in an open-shell singlet (**Cu1S″**), and (3) a closed-shell, in-plane sp^2 hybrid singlet with the p_z orbital unfilled (**Cu1S‴**). Based on ketocarbene electrophilicity and orbital symmetry arguments, this latter intermediate is not thought to contribute to product formation from photolysis of diazo-oxochlorins, *unless a considerable structural distortion occurs during the reaction trajectory*. Based on this premise, the electronic structures and directionalities of the other two states must lead to three reactions (pathways a−c) that account for the major products isolated upon photolysis of **Cu1**. Ketocarbenes are known to undergo Wolff rearrangement (pathway a) and insert into chemical bonds (pathway b), as well as to participate in H-atom abstraction reactions (pathway c). Pathway a requires that the unoccupied sp^2 orbital of **Cu1S′** lie in the plane of the chlorin ring to promote ring contraction, while intramolecular insertion into the *meso*-phenyl ring, pathway b, could conceptually derive from either **Cu1S′** or **Cu1S″** (*vide infra*).

Experimentally, broadband photolysis ($\lambda \geq 345$ nm) of both free-base and metalated diazo-oxochlorins leads to formation of the unusual Wolff ring-contracted photoproducts via substrate addition (pathway a). This suggests that the electronic structures

(68) Nazran, A. S.; Griller, D. *J. Am. Chem. Soc.* **1984**, *106*, 543.
(69) Tomioka, H.; Hirai, K.; Nakayama, T. *J. Am. Chem. Soc.* **1993**, *115*, 1285.

and local periphery polarizations of the corresponding carbene intermediates are very similar. Since the high-energy **Cu1S′** intermediate has a vacant back lobe of the sp^2 hybrid orbital in the plane of the pyrrole ring, donation from the adjacent C−C σ-orbital to the electron-deficient carbene facilitates the Wolff rearrangement.[70]

Along pathway b, both structurally characterized photoproducts, **Cu4** and free-base derivative **H5**, show exocyclic ring formation, which also results from electrophilic attack/insertion by the deficient sp^2 orbital. For this primary step, two possible routes are viable. The first involves insertion of the electron-deficient orbital into the C−H bond at the *ortho* position of the transiently planar ring, as is customary for carbene insertion into aliphatic hydrocarbons.[42,43] The second is defined by electrophilic attack upon the π-system of the *meso*-phenyl ring.[71] For a bimolecular event, the latter pathway is likely preferred; however, in the constrained geometry of the macrocycle, $sp^2-\pi$ (phenyl) orbital overlap is compromised due to the requirement for partial ring rotation to relieve orthogonality. This leaves the precise mechanism for exocyclic ring formation somewhat ambiguous based solely on product distribution.

Under this general scheme, electrophilic attack on the *meso*-phenyl ring by the carbene leads to transient radical formation on both the macrocycle and the compromised phenyl ring. For the metalated chlorins (e.g., **Cu4**), H-atom migration to the macrocycle re-aromatizes the phenyl ring and generates the keto-chlorin product. This species can then undergo a keto−enol tautomerization[72] to yield the isolated exocyclic ring-containing hydroxyl species **Cu4**. In contrast, for the free-base derivative, loss of an H-atom (macroscopically as H_2) re-aromatizes the ring, producing a monoradical on the macrocycle that can undergo bimolecular radical−radical coupling to yield homodimer **H5**. The sensitivity of the keto−enol tautomerization to the presence of central metal ion (*vide infra*)[72] may be a differentiation point between these products.

Within the theme of the radical reactivity above, the locally separated but spin-paired electrons of the open-shell singlet of **Cu1S″** can also participate in triplet carbene-like reactivity (i.e., H-atom abstraction) with substrate, resulting in the hydroxylated products **Cu3** of pathway c. Despite the apparent insensitivity of product formation to the central metal for pathways a and b, it is well known that π-electron distribution across the macrocycle can play an important role in the reactivity of the porphyrinoid periphery.[73] For instance, the relatively electronegative metal ions, Cu(II) and Ni(II), have been shown to function as activating groups for nucleophilic reactions at the porphyrin periphery.[74] For metalated 2-hydroxy-5,10,15,20-tetraphenylporphyrins (e.g., **Cu3**), this results in a dramatic difference in the keto−enol tautomer equilibrium relative to the corresponding free base, even in the solid state.[72,75] Here, the Cu(II) and Zn(II) analogues were found to exist almost exclusively as hydroxyporphyrins.[72] On the basis of this detailed report, we propose that such a keto−enol equilibrium is also operative during the photochemical reaction of the open-shell singlet diradical (**Cu1S″**) of these diazo-oxochlorins. The supposition is supported by the observation that only metalated diazo-oxochlorins form hydroxylated products such as **Cu3** and **Ni3**, while the corresponding free-base analogue is never observed.

Although the reaction pathways described in Scheme 2 provide a qualitative understanding of the possible origins of the different photoproducts, they do not give information about the energetics of the intermediate or address what drives the product distribution. Pathways a and c are clearly influenced by substrate. The presence of a nucleophilic solution substrate channels reactivity toward isolable Wolff product, albeit in modest yields (∼10−30%). Under these same substrate conditions (Table 1), significant quantities of hydroxyporphyrin (∼5−35%) are also obtained, deriving pathway c, whereas in the absence of nucleophilic substrate, intramolecular quenching by addition to the *meso*-phenyl ring (pathway b) dominates (66−76%). The ability of the substrate to trap the Wolff-rearranged ketene and the hydroxypophyrin via **Cu1S′** and **Cu1S″**, respectively, leads to their presence as isolable products. Interestingly, although both substrate-dependent pathways a and c appear inoperative in the absence of nucleophile, it is the phenyl ring addition and hydroxyporphyrin products, from pathways b and c, respectively, that most obviously compete based on product yields (cf. Table 1, expts 5−8), with the Wolff species appearing somewhat invariant under substrate conditions. In light of this chemical interplay, we attribute reaction pathway b and intramolecular exocyclic ring formation to intermediate **Cu1S″**.

Since **Cu1** is formally reduced during transformation to **Cu3** along pathway c, we postulated that substrate *oxidation* may be the key parameter required for generation of **Cu3**. This would explain why formation of **Cu3** is diminished during photolysis in neat dichloromethane. To support this hypothesis, **Cu1** was photolyzed in the presence of *tert*-butyl alcohol. Since tertiary alcohols are more resistant to oxidation and are generally less nucleophilic, formation of **Cu3** should be limited. In fact, photolysis of **Cu1** in the presence of *tert*-butyl alcohol under conditions similar to those described for substrates **a**−**c** gave no **Cu3** and instead gave the intramolecular phenyl addition product **Cu4** in 51% yield, mirroring the result obtained in the absence of substrate. This strongly suggests that the major driving force for reaction pathway c in Scheme 2 is the tendency of the substrate toward oxidation. Therefore, reduction of the photogenerated carbene porphyrinoid with subsequent keto−enol tautomerization must account for the formation of **Cu3**. To further support this conclusion, **Cu1** was photolyzed in the presence of the non-nucleophilic reducing agent 1,4-cyclohexadiene, which should enhance the formation of **Cu3** if the proposed mechanism is valid. Indeed, photolysis of **Cu1** in the presence of 1,4-cyclohexadiene gives 55% yield of **Cu3** and no **Cu4**. These results lead to the conclusions that the photoprepared carbene intermediates are capable of substrate oxidation and the observed photoproduct ratios are related to the oxidation potential of the specific substrate.

Finally, photolysis of **Cu1** in aqueous media containing 16:0 PEG3 PE micelles reveals isosbestic conversion of **Cu1** to one major product at 10 °C, which is in great contrast to the more diverse photochemical decay of **Cu1** in dichloromethane under similar conditions (Figure 7). Micelle encapsulation is certainly expected to diminish the possibility of dimer formation, which is in agreement with the observed spectroscopic data for the

(70) McMahon, R. J.; Chapman, O. L.; Hayes, R. A.; Hess, T. C.; Krimmer, H. P. *J. Am. Chem. Soc.* **1985**, *107*, 7597.
(71) Abramovitch, R. A.; Alexanian, V.; Smith, E. M. *J. Chem. Soc., Chem. Commun.* **1972**, 893.
(72) Crossley, M. J.; Harding, M. M.; Sternhell, S. *J. Org. Chem.* **1988**, *53*, 1132.
(73) Catalano, M. M.; Crossley, M. J.; Harding, M. M.; King, L. G. *J. Chem. Soc., Chem. Commun.* **1984**, 1535.
(74) Crossley, M. J.; King, L. G.; Pyke, S. M. *Tetrahedron* **1987**, *43*, 4569.
(75) Crossley, M. J.; Field, L. D.; Harding, M. M.; Sternhell, S. *J. Am. Chem. Soc.* **1987**, *109*, 2335.

photolyzed micelle solution. More specifically, based upon electronic spectral analysis, R_f value comparison, and mass spectroscopy after photolysis, sequestration appears to drive the reaction along pathway c, forming **Cu3**, likely via oxidation of the micelle by **Cu1S″**.

Conclusion

Photolysis of diazo-oxochlorins leads to pyrrole ring contraction and substrate trapping (Wolff rearrangement) of the rare azeteoporphyrinoids via the spin-paired singlet carbene, while the open-shell singlet state leads to unusual exocyclic ring formation and substrate oxidation by H-atom abstraction, generating hydroxyporphyrin products. Choice of reaction pathway is to some extent under substrate control, providing a manifold for variable chemical reactivity. Aqueous photochemistry is also realized upon micelle encapsulation of the starting diazo-oxochlorin, where the products are once again driven by the environment of the micelle interior. In general, the ability to influence and modulate substrate addition, alkylation, or oxidation using these photoreactive chromophores leads to potential for such constructs as biological labeling or damaging motifs in the absence of co-reagents or O_2.

Acknowledgment. The support of Indiana University and the Argonne National Laboratory is gratefully acknowledged. ChemMatCARS Sector 15 is principally supported by the National Science Foundation/Department of Energy under grant number CHE-0535644. Use of the Advanced Photon Source was supported by the U.S. Department of Energy, Office of Science, Office of Basic Energy Sciences, under Contract No. DE-AC02-06CH11357.

Supporting Information Available: Details about X-ray structure data collection, structure solution, and refinement for **Cu2a**−**c**, **H2a**, **Cu4**, and **H5**, including CIF files. This material is available free of charge via the Internet at http://pubs.acs.org. The crystallographic data for the structures reported herein have been also deposited with the Cambridge Crystallographic Data Centre as CCDC Nos. 668799 (**Cu4**), 668800 (**H2b**), 668801 (**Cu2b**), 668802 (**H5**), 668803 (**Cu2a**), and 668804 (**Cu2c**). Copies of the data can be obtained free of charge on application to CCDC, 12 Union Rd., Cambridge CB2 1EZ, UK (fax (+44) 1223-336-033; E-mail deposit@ccdc.cam.ac.uk).

JA800094E